

S.Y. WANG  
B.L. CHENG<sup>✉</sup>  
C. WANG  
S.Y. DAI  
H.B. LU  
Y.L. ZHOU  
Z.H. CHEN  
G.Z. YANG

# Mechanisms of asymmetric leakage current in Pt/Ba<sub>0.6</sub>Sr<sub>0.4</sub>TiO<sub>3</sub>/Nb-SrTiO<sub>3</sub> capacitor

Beijing National Laboratory for Condensed Matter Physics, Institute of Physics,  
Chinese Academy of Sciences, Beijing 100080, P.R. China

Received: 26 February 2004 / Accepted: 21 July 2004

Published online: 31 August 2004 • © Springer-Verlag 2004

**ABSTRACT** Mechanisms of leakage current have been investigated in the capacitor consisting of a Ba<sub>0.6</sub>Sr<sub>0.4</sub>TiO<sub>3</sub> thin film, a Pt top electrode, and a Nb-doped SrTiO<sub>3</sub> (STON) bottom electrode. The leakage current shows asymmetric behavior for different bias voltage. For the Pt electrode negatively biased, the leakage current can be explained by modified Schottky emission mechanism, and the barrier height is obtained as 0.44 eV. For the Pt electrode positively biased, the leakage current shows a space-charge-limited current behavior. The trap in dielectric film is regarded as deep traps, and the density of trapped carrier is estimated as about  $3.2 \times 10^{23}/\text{m}^3$ .

PACS 77

## 1 Introduction

Thin films of Ba<sub>1-x</sub>Sr<sub>x</sub>TiO<sub>3</sub> (BST) have recently been received considerable attention as promising candidates for applications in tunable microwave devices and in dynamic random access memories [1–3]. It is well documented that, in a form of capacitor, the electrical and reliability properties are strongly influenced by the electrode. The electrode studied so far can be classified into three groups. The first group consists of noble metals, such as Pt, Au, Ru and Ir [1, 2, 4, 5]. The second group consists of rutile-type metal oxides, such as RuO<sub>2</sub> and IrO<sub>2</sub> [4, 6]. The third group of electrode materials is the conducting perovskite oxide electrodes, such as LaNiO<sub>3</sub>, SrRuO<sub>3</sub> and Nb-doped SrTiO<sub>3</sub> (STON) [8–12], which have same crystal structure as the dielectric BST. Earlier studies have shown that the noble metals usually form a Schottky contact with BST, thus limiting the leakage current and gave excellent electrical properties. The proposed leakage mechanisms in the capacitor with noble metal include Schottky emission [1], Poole–Frenkel emission [12], modified Schottky emission [2], and space-charge-limited current (SCLC) [1], etc. Unfortunately, there exist serious shortcomings with noble metal, including etching difficulty and high oxygen permeability, which results in the formation of oxygen vacancy, accelerating the degradation of the dielectric

properties of BST thin film [13]. Studies have demonstrated that the rutile-structure oxide electrodes do not form blocking contacts to BST, but the leakage current densities in capacitors with oxide electrodes were higher than that with noble metal [4, 6]. It is proposed that transport in IrO<sub>2</sub>/BST/IrO<sub>2</sub> capacitor is through bulk-limited, and Poole–Frenkel emission is responsible for the leakage mechanism [13]. The third class of electrodes, namely the perovskite oxide electrodes, has inherent advantage that they are well lattice matched with BST, thus promoting phase stability of the dielectric layer. Watanabe et al. reported some investigations on the BaTiO<sub>3</sub> thin film prepared on STON bottom electrode, such as reproducible memory effect in leakage current, the difference between the characteristics of nanometer and millimeter-size metal contacts, and nonlinear positive temperature coefficient of resistance, etc. [10–12]. Recently, we have investigated the dielectric property of BST epitaxial thin films deposited on single-crystal STON substrate [3]. Furthermore, we reported a reduction of leakage current by Co-doping in Pt/BST/STON capacitor in the condition of Pt positively biased. In order to fully understand the fundamental mechanisms for leakage current in different bias, in this study, the characteristics of the leakage current versus applied bias voltage (*I*–*V*) in asymmetric Pt/BST/STON capacitor have been investigated in the whole bias range, and possible mechanisms for the leakage current are discussed.

## 2 Experiments

The BST ceramic target with a diameter of 25 mm and a thickness of 4 mm were prepared by conventional solid-state reaction using analytic reagent grade of purity [3]. The (001) STON substrate with a thickness of about 0.5 mm and a surface of  $3 \times 5 \text{ mm}^2$  had been cleaned with alcohol and acetone in an ultrasonic bath, the BST thin films were deposited onto them with pulsed-laser deposition (PLD) technique employing a XeCl excimer laser (308 nm, 20 ns and 4 Hz). A laser with energy density of about  $2 \text{ J/cm}^2$  was focused on the ceramic target mounted on a motor-driving rotary shaft rotating at a constant speed to ensure a uniform ablation rate. The STON substrate was maintained at 800 °C for 20 min, the deposition of the BST thin film were carried out at the same temperature in a oxygen pressure of 0.2 Pa. After deposition the thin films were annealed at 800 °C for 10 min

✉ Fax: +86-10/8264-9531, E-mail: blcheng@aphy.iphy.ac.cn

under oxygen pressure of 500 Pa. The thickness of BST thin films was measured as 160 nm by a surface profile measuring system (DEKTAK □, U. S. A.).

The crystalline phase and structure of the BST thin films were analyzed by X-ray diffraction (XRD) using Cu  $K_{\alpha}$  radiation (40 kV, 50 mA) and a graphite monochromator. The surface morphologies of the BST thin films were observed with Nano Scope III atomic force microscopy (AFM). For electrical measurements, Pt top electrodes with a diameter of 0.2 mm were deposited through a shadow mask onto the BST thin films under the pressure of  $1 \times 10^{-3}$  Pa at room temperature. The leakage current was measured with a RT-6000S ferroelectric test system, with the bottom electrode STON grounded.

### 3 Results and discussions

The XRD profile of BST thin films deposited on STON substrates shows only (001) peaks for both films and substrates, indicating that BST thin films are aligned along (001) direction, normal to the substrate surface. The surface morphology of the film was smooth with no cracks and defects, and the smoothness of the surfaces, measured as root-mean-square surface roughness  $R_{\text{rms}}$ , is smaller than  $2 \text{ \AA}$ .

The leakage current versus applied bias voltage is shown in Fig. 1. The  $I$ - $V$  curves show conventional diode characteristics. Similar results have been reported previously on Pt/BaTiO<sub>3</sub>/STON [10–12]. The diode characteristic of the  $I$ - $V$  curve maybe originates from the variation of the leakage mechanism, resulted from the different contact interfaces of Pt/BST and STON/BST. In order to determine the mechanism of leakage current, Current-voltage characteristics on a logarithmic scale and the slope of the  $\log(I)$  versus  $\log(V)$  curve are plotted in Fig. 2a and b, respectively, providing the information about the conduction mechanism. It is shown that the ratio of  $d(\log(I))/d(\log(V))$  can be divided into four regions. In region I, the ratio of  $d(\log(I))/d(\log(V))$  varies from 6.0 to 4.0; in region II, the ratio is around 1.0; in region III, the ratio varies from 2.0 to 9.2; in region IV, the ratio is about 2.5. In region I the leakage current is probably dominated by Schottky emission because the ratio is larger than 4; and in low bias region the leakage current demonstrate Ohmic law due to the slope near 1. However, in region III and IV leakage conduction at first increases rapidly and then increases mildly.

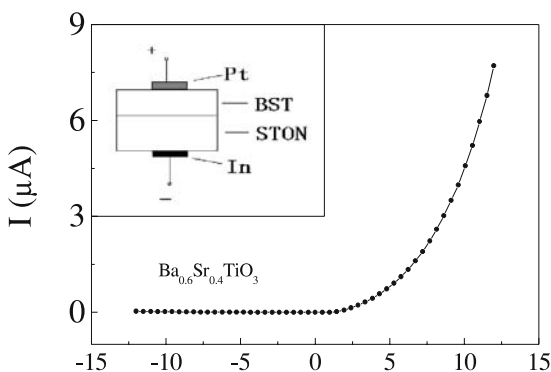


**FIGURE 1**  $I$ - $V$  characteristic of the Pt/BST/STON capacitor. The inset shows the schematic diagram of the capacitor

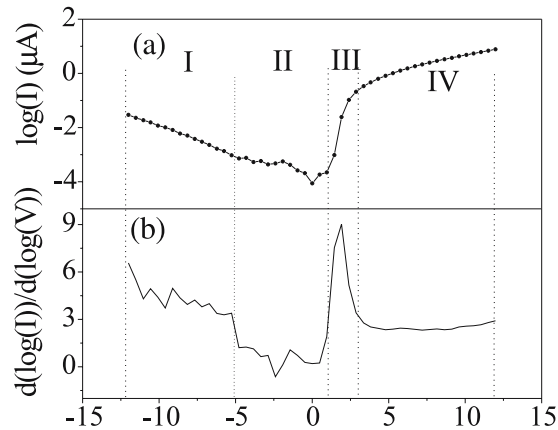


**FIGURE 2** Current-voltage characteristics on a logarithmic scale (a) and slope of the  $\log(I)$ - $\log(V)$  curve (b) of the Pt/BST/STON capacitor

When the top Pt electrode is negatively biased, the Schottky barrier formed between Pt electrode and BST dielectric thin film is probably responsible for the leakage mechanism, as illustrated in Pt/BST/Pt capacitor [1, 2]. In modified Schottky equation, the current density  $J$  can be written as [3]:

$$J = a\mu_e T^{3/2} E (m^*/m_0)^{3/2} \times \exp \left[ -\Phi_t + (q^3 E / 4\pi\epsilon_0\epsilon)^{1/2} / kT \right], \quad (1)$$

where  $\mu_e$  is the electron mobility in BST,  $T$  the absolute temperature,  $E$  the applied electric field,  $m^*$  the effective electron mass,  $m_0$  the free-electron mass,  $\Phi_t$  the Schottky barrier height at the Pt,  $q$  the electronic charge,  $\epsilon_0$  the permittivity of free space,  $\epsilon$  the optical dielectric constant,  $k$  the Boltzmann constant, and  $a$  is a constant and can be assume as  $3 \times 10^{-4} \text{ As/cm}^3 \text{ K}^{3/2}$  [3]. If the conduction current is governed by modified Schottky emission, the  $\ln(J/E)$  versus  $E^{1/2}$  plot should be a straight line and the slope will give the optical dielectric constant, which is about 4.0 according to the square of the refractive index  $n$  [15]. In Fig. 3,  $\ln(J/E)$  is plotted versus  $E^{1/2}$  for the leakage current in the case of Pt negatively biased ( $0 \rightarrow -12 \text{ V}$ ). It is shown that when the  $E$  is higher than about  $160 \text{ kV/cm}$  ( $E^{1/2} > 400 \text{ V}^{1/2} \text{ cm}^{1/2}$ ), the modified Schottky equation provides a good fit, as indicated by the

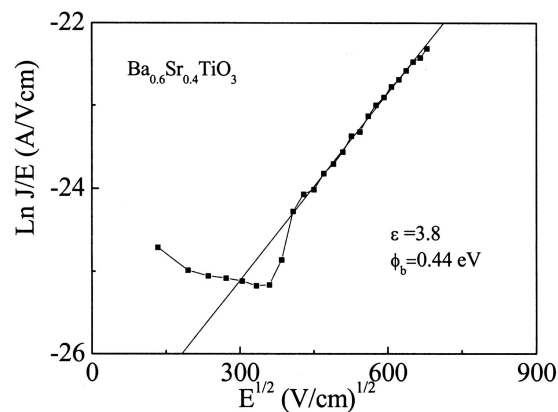


**FIGURE 3** Modified Schottky emission plot of  $\ln(J/E)$  vs.  $E^{1/2}$  under negative bias ( $0 \rightarrow -12 \text{ V}$ ) on Pt electrode. The optical dielectric constant and the barrier height calculated are 3.8 and 0.44 eV, respectively

straight solid line. The slope of the fit line provides an estimation of the optical dielectric constant ( $\epsilon$ ), and  $\epsilon$  is thereby estimated as 3.8. Such value of  $\epsilon$  agrees well with the optically determined value of about 4.0 [15]. Hence the modified Schottky equation provides a satisfactory description of the  $\epsilon$ . Furthermore, with  $m^* = 5 m_0$  and  $\mu = 0.001 \text{ cm}^2/\text{Vs}$  [15], the Schottky barrier height  $\Phi_t$  can be calculated as 0.44 eV.

Figure 4 shows a log-log plot of the leakage current versus the applied voltage with the Pt electrode biased with positive bias voltage. The slope is about 0.5 in the low voltage region; it is followed by a transition region characterized by a large slope; at higher bias above 2.3 V, the slope of  $\log(I)$  versus  $\log(V)$  plot is about 2.4. Such characteristics agree well with the space-charge-limited current (SCLC) theory with traps [2, 14]: the region 1 follows Ohm's law for the ratio of  $\log(I)/\log(V)$  near 1.0. Due to the ferroelectric polarization and strong voltage-dependence of dielectric constant at grain boundaries, the slope in low electric field is usually less than 1, as shown in Fig. 4 [9, 16]; the region 2 corresponds to the accomplishment of the trap-filling process, and then gives a sharp increase of the leakage current; the region 3 corresponds to the trap-free square law with self-blockage of charge carriers. The conduction current ( $J$ ) at high bias region from SCLC theory can be expressed as the following form [14].

$$J = 9\epsilon_r\epsilon_0\mu_e V^2/8d^3, \quad (2)$$

where  $V$  is the bias voltage,  $\epsilon_r$  the permittivity of the thin film, and  $d$  the thickness of thin film. Figure 4 shows that the TFL characteristic is merged into the trap-free square law when  $V \approx 2V_{\text{TFL}}$ , therefore, the trap in the dielectric film can be regarded to be deep traps, namely, the trap located below the Fermi level in the energy gap [14]. At that point  $V \approx 2V_{\text{TFL}}$ , the free space charge begins to exceed and overshadow the trapped space charge. The trapped electron density ( $N_t$ ) can be calculated from the trap-filled limit voltage ( $V_{\text{TFL}}$ ) using [1, 2]

$$N_t = 9\epsilon_r\epsilon_0 V_{\text{TFL}}/8qd^2. \quad (3)$$

Experimentally,  $V_{\text{TFL}}$  in region 2 obtained from Fig. 4 are about 1.2 V. Then the value of  $N_t$  at room temperature can be calculated as about  $3.2 \times 10^{23}/\text{m}^3$ .

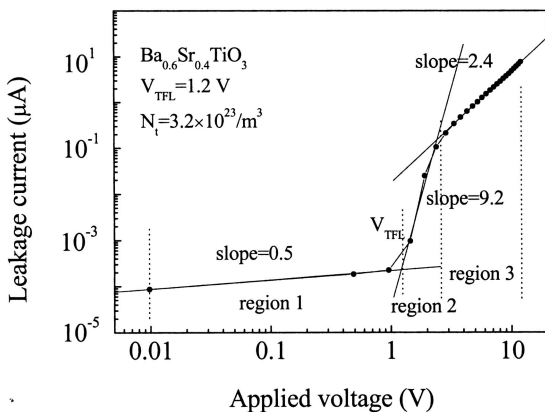


FIGURE 4 Logarithm of the current plotted as a function of the logarithm of the applied voltage at positive bias (12 → 0 V) on Pt electrode

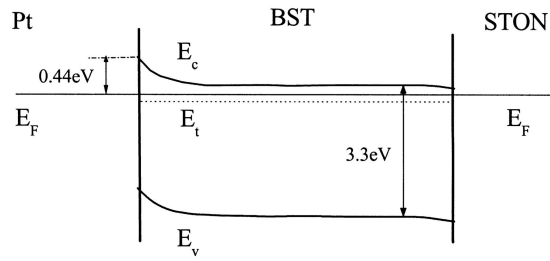


FIGURE 5 Schematic energy band of the Pt/BST/STON capacitor without bias voltage

From the above phenomenological analysis of the leakage current, the modified Schottky emission model and SCLC theory are responsible for the leakage mechanism in the Pt/BST/STON capacitor for the negative and positive bias, respectively. Based on the above results, a schematic energy band of the Pt/BST/STON capacitor is proposed, as shown in Fig. 5. It is suggested that the injection of conduction electrons from the top electrode (Pt) to the BST is performed under the negative bias on the Pt, and that from the bottom electrode (STON) to the BST is performed under the positive bias on the Pt electrode [1]. At the low oxygen pressures in the preparation of BST thin films, BST can be considered as an n-type semiconductor due to the dominant defect formed by oxygen deficiency [17]. When the semiconductor is contacted with Pt, Schottky diode is constructed based on the well-established metal/semiconductor contact theory [18]. For the Pt/BST/Pt capacitor, it is suggested that two Schottky diode connected back to back in the Pt/BST/Pt capacitor. There is always an electrode is biased negatively in despite of the polarity, resulting in the symmetrical behavior of  $I-V$  curves. However, for the Pt/BST/STON capacitor, when Pt is negatively biased, the electron injected from the Pt electrode is impeded by the Schottky barrier at the interface of Pt and BST thin film, as shown in Fig. 5; but when Pt is positively biased, the Schottky barrier becomes conductive enough for the electron injected from the bottom electrode STON into the BST thin film [14], then the SCLC current mechanism dominates the leakage current. In the low bias region, the ohmic-like current behavior dominates; the slope of  $I-V$  curve is smaller than 1.0, which probably resulted from the ferroelectric polarization of BST thin film [9, 16]. In the higher bias region, after the filling of the deep traps at  $V_{\text{TFL}}$ , the leakage current increases sharply, following by the trap-free square law with self-blockage of charge carriers. The different leakage mechanism implies the different contact nature in the Pt/BST and STON/BST interfaces. When the BST contacts with STON electrode, most of the surface dangling bond will disappear; but when the BST contacts with Pt, the chemical states of the surface dangling bonds can be preserved after contact formation, resulting in the upward band bending due to the Fermi level pinning as illustrated by Hwang et. al [7]. Such difference results in different mechanisms of leakage current in Pt/BST/STON capacitor.

#### 4 Conclusions

The leakage current in Pt/BST/STON capacitor demonstrates an asymmetric behavior at positive and negative

bias. When the Pt electrode negatively biased, the electrons are injected from Pt to STON through BST, and the leakage current can be explained by modified Schottky emission mechanism at the Pt/BST interface, and the Schottky barrier height is calculated as 0.44 eV. When the Pt electrode is positively biased, the conduction electrons are transformed from STON to Pt through BST film, and the leakage current seems to be controlled by space-charge-limited current mechanism. The trapped electron density was estimated as  $3.2 \times 10^{23}/\text{m}^3$ .

**ACKNOWLEDGEMENTS** The work was supported by the “Hundreds Talents Project” of the Chinese Academy of Sciences and the National Natural Science Foundation of China.

## REFERENCES

- 1 H. Yang, B. Chen, K. Tao, X.G. Qiu, B. Xu, B.R. Zhao: Appl. Phys. Lett. **83**, 1611 (2003)
- 2 K. Tao, Z. Hao, B. Xu, B. Chen, J. Miao, H. Yang, B.R. Zhao: J. Appl. Phys. **94**, 4042 (2003)
- 3 S.Y. Wang, B.L. Cheng, C. Wang, H.B. Lu, Y.L. Zhou, Z.H. Chen, G.Z. Yang: J. Cryst. Growth **259**, 137 (2003)
- 4 J. Bandaru, T. Sands, L. Tsakalacos: J. Appl. Phys. **84**, 1121 (1998)
- 5 K.B. Lee, S. Tirumala, S.B. Desu: Appl. Phys. Lett. **74**, 1484 (1999)
- 6 H.N. Al-Shareet, O. Auciello, A.I. Kingon: J. Appl. Phys. **77**, 2146 (1995)
- 7 C.S. Hwang, B.T. Lee, C.S. Kang, J.W. Kim, K.H. Lee, H.J. Cho, H. Horii, W.D. Kim, S.I. Lee, Y.B. Roh, M.Y. Lee: J. Appl. Phys. **83**, 3703 (1998)
- 8 M.S. Chen, T.B. Wu, J.M. Wu: Appl. Phys. Lett. **68**, 1430 (1996)
- 9 X.D. Fang, T. Kobayashi: J. Appl. Phys. **90**, 160 (2001)
- 10 Y. Watanabe: Appl. Phys. Lett. **66**, 28 (1995)
- 11 Y. Watanabe, D. Sawamura, M. Okano: Appl. Phys. Lett. **72**, 2415 (1998)
- 12 M. Okano, Y. Watanabe, S.W. Cheong: Appl. Phys. Lett. **82**, 1923 (2003)
- 13 K. Morito, T. Suzuki, S. Sekiguchi, H. Okushi, M. Fujimoto: Jpn. J. Appl. Phys. **39**, 166 (2000)
- 14 M.A. Lampert: Phys. Rev. **103**, 1648 (1956)
- 15 S. Zafar, R.E. Jones, B. Jiang, B. White, V. Kaushik, S. Gillespie: Appl. Phys. Lett. **73**, 3533 (1998)
- 16 C.J. Peng, S.B. Krupanidhi: J. Mater. Res. **10**, 708 (1995)
- 17 K.H. Ahn, S. Baik, S.S. Kim: J. Appl. Phys. **92**, 2651 (2002)
- 18 S.M. Sze: *Physics of Semiconductor Devices*, 2nd edn. (Wiley, New York 1981)